Effect of titanium content on solidification structure of ferritic stainless steel gas–tungsten and gas–metal arc welds

by L.S. Linda*[1] and P.G.H Pistorius[1]

*Paper written on project work carried out in partial fulfilment of BEng (Metallurgical Engineering) degree

Affiliation:
[1]Department of Materials Science and Metallurgical Engineering, University of Pretoria, Pretoria, South Africa.

Correspondence to:
P.G.H. Pistorius

Email:
pieter.pistorius@up.ac.za

Dates:
Received: 13 Dec. 2021
Accepted: 23 Feb. 2022
Published: July 2022

How to cite:
Linda, L.S. and Pistorius, P.G.H. 2022 Effect of titanium content on solidification structure of ferritic stainless steel gas–tungsten and gas–metal arc welds. Journal of the Southern African Institute of Mining and Metallurgy, vol. 122, no. 7, pp. 331–336

DOI ID:
http://dx.doi.org/10.17159/2411-9717/1944/2022

ORCID:
P.G.H. Pistorius
https://orcid.org/0000-0001-6582-8157

Synopsis

Ferritic stainless steel is utilized to fabricate automotive exhaust systems using a ferritic weld metal. Ductility of the weld metal is higher if its microstructure contains a significant proportion of equiaxed grains. The formation of equiaxed (rather than columnar) grains is favoured by a higher titanium weld metal content. In this study, the Ti content of ferritic stainless steel weld metal was changed by using Ti-free (Type 436) and Ti-containing (441) ferritic stainless steel as base metals. The metal-cored welding consumable contained 0.4% Ti. Gas–tungsten arc welding and gas–metal arc welding processes were compared. The weld metal Ti content ranged from zero to 0.5% Ti, as determined from scanning electron microscopy supplemented by inductively coupled plasma optical emission spectroscopy. Cross-sections of the weld beads were subjected to point counting (to estimate the fraction of equiaxed grains) and image analysis (to estimate the average grain size). Point counting proved to be more reliable. The fraction of equiaxed grains was sensitive to the Ti content, but not to the welding process. Below 0.4% Ti, the fraction of equiaxed grains gradually increased with an increase in the weld metal Ti content; above 0.4% Ti, the fraction of equiaxed grains rapidly increased with increasing Ti content. The transition in behaviour at 0.4% Ti corresponded to a Ti content at which Ti-rich precipitates became stable at the estimated liquidus temperature of the weld metal.

Keywords

ferritic stainless steel, fusion welding, solidification structure, columnar-to-equiaxed transition, titanium.

Introduction

Ferritic stainless steels, often alloyed with Ti, Nb, Mo, or some combination of these elements, are used to fabricate automotive exhaust systems. The fabrication process involves manufacturing longitudinally welded tubes that are often subsequently plastically deformed. For this reason, the welded joint must have adequate ductility. Given the cyclic nature of the temperature of an exhaust system and the high peak temperatures encountered, the weld metal is usually ferritic to avoid dissimilar thermal expansion, which is inherent in the use of an austenitic welding consumable. Ferritic weld metal is inherently less ductile than an austenitic material, so it is more difficult to achieve adequate ductility. One precondition for ferritic weld metal with adequate ductility is a solidification structure that is dominated by equiaxed grains (Villafuerte, Pardo, and Kerr, 1990).

The solidification of ferritic stainless steel weld metal starts by epitaxial solidification, *i.e.*, growth of unmelted grains (in the high-temperature heat-affected zone) into the weld pool, resulting in large columnar grains. Under specific conditions, equiaxed grains may form closer to the centre line of the weld pool (Lippold, 2014). The columnar–equiaxed transition (CET) is sensitive to, among other parameters, the Ti content of the weld metal. Villafuerte, Pardo, and Kerr (1990) reported autogenous gas–tungsten arc welding (GTAW) beads on five Type 409 ferritic stainless steels (with about 11% Cr). The welding speed was varied from 3 to 14 mm/s. The fraction of equiaxed grains in the weld metal was measured on the top surface of the weld. A low welding speed resulted in a low fraction of equiaxed grains. Once the Ti content exceeded a threshold value of about 0.18%, the fraction of equiaxed grains increased with a higher Ti content. Metallographic evidence of the role of Ti-containing particles in nucleating equiaxed grains was presented. Villafuerte, Kerr, and David (1995) confirmed the role of TiN

particles in nucleating equiaxed grains by quenching stationary GTAW beads with liquid tin. Villaret *et al.* (2013a) used gas–metal arc welding (GMAW) to deposit weld beads on a Grade 444 ferritic stainless steel (19% Cr, 2% Mo, 0.6% Nb) using various metal-cored welding consumables. The Ti content of the weld metal varied from 0.045% to 0.35%. The fraction of equiaxed grains in the weld metal was measured on a cross-section of the weld, presumably sampling the complete weld bead. A Ti content of 0.15% resulted in weld metal that was fully equiaxed. Villaret *et al.* (2013b) subsequently confirmed these results and noted that an equiaxed weld metal structure could accommodate some plastic deformation.

Villaret, Deschaux-Beaume, and Bordreuil (2016) developed a solidification model for the CET in Ti-containing ferritic stainless steels. The volume fraction of Ti-rich precipitates was considered to play an important role in the CET: weld metal, with higher Ti content contained more and larger Ti-rich precipitates. Prins (2020) reported the effect of autogenous GTAW parameters on the fraction of equiaxed grains in the weld metal of two ferritic stainless steels: Type 436 (with no Ti) and Type 441 (containing 0.18% Ti). The fraction of equiaxed grains in more than 200 welded joints were reported. No combination of welding parameters resulted in the formation of equiaxed grains in the Type 436 weld metal; for the Type 441 weld metal, the fraction of equiaxed grains varied from approximately 0.2 to approximately 0.8, with no clear effect of welding parameters or combination of welding parameters.

All these results, which strictly speaking are not fully comparable owing to differences in the base metal composition, are summarized in Figure 1. No study reported a systematic change in weld metal Ti content and it is not clear whether the fraction of equiaxed grains in the weld metal was sensitive to the welding process. GMAW generally resulted in a higher fraction of equiaxed grains in the weld metal for the same Ti content, but the fraction of equiaxed grains varied significantly at a given Ti content. The aim of the current study was therefore to systematically change the weld Ti content, using two welding processes and two base metal compositions, so as to determine if the fraction of equiaxed grains in ferritic stainless steel weld metal is sensitive to the welding process or only to the Ti content.

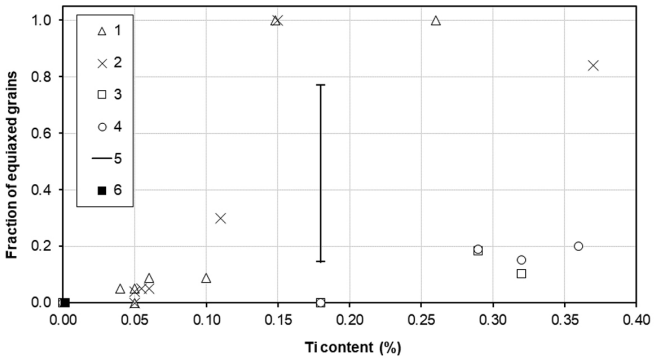

Figure 1—Published data on the effect of weld metal Ti content on the fraction of equiaxed grains in different grades of ferritic stainless steel weld metals (key to data: 1: pulsed GMAW Villaret *et al.*, 2013a; 2: short circuit GMAW, Villaret, *et al.*, 2013a, 3: GTAW 3 mm/s Villafuerte, Pardo, and Kerr, 1990; 4: GTAW 14 mm/s Villafuerte, Pardo, and Kerr, 1990; 5: Grade 441 Prins, 2020, 6: Grade 436: Prins, 2020)

Experimental procedure

Welding parameters

Two ferritic stainless steel base metals were used: Grade 436 (a Mo-containing steel with no intentional Ti addition) and Grade 441 (with nominally 0.2% Ti). Compositions are shown in Table I. A metal-cored welding consumable with a nominal Ti content of 0.4% was used. The plate thickness was 1.5 mm (Grade 436) or 1.2 mm (Grade 441). The base metal was cut into strips with a width of 50 mm and wiped down with alcohol to remove oil, dust, and other surface impurities before welding. Two welding processes were used: GTAW and GMAW. For the GTAW, two welds were autogenous (without filler wire); for the rest of the GTAW beads the metal-cored filler wire was used with a range of welding currents and wire feed speeds. Pure argon was used as the shielding gas. The welding speed was approximately 5 mm/s. Typical of industrial practice, the wire feed was pulsed. A constant current programme was used (program 375 on the Lincoln Electric S350 Power Wave welding power supply). For the GMAW, the wire feed speed, welding current, and welding speed were varied to achieve full penetration welds, using pulsed-spray transfer with an Ar–2% O_2 shielding gas. For both processes, pure Ar backing gas was used. The welding parameters for both processes are noted in Table II. Wide ranges of welding speeds and currents were used. Given the objective to achieve full-penetration welded joints on thin sheet, the heat input was low and did not vary significantly.

Characterization of weld metal

Samples were sectioned transverse to the weld, hot mounted, ground, polished to a 1 µm finish, and etched using Villella's reagent (1 g picric acid, 5 ml hydrochloric acid, and 100 ml ethanol). Energy-dispersive X-ray spectroscopy scanning microscopy (SEM–EDS, JEOL JSM-IT300, Japan, equipped with Aztec software) was employed to determine the chemical composition of the base and weld metals. In addition, several welds were removed by sectioning and submitted for analysis using inductively coupled plasma optical emission spectroscopy (ICP–OES).

The fraction of equiaxed grains in the weld metal was determined by two techniques: manual point counting and image analysis. A monotone image of the grain boundaries of each

Table I

Chemical compositions (mass%) of Type 436 and Type 441 base metal and T439Ti metal-cored welding consumable, as certified by supplier

	Cast number	C	Si	Mn	Ni	Cr	Mo	Nb	Ti
436 base metal	4212173	0.01	0.39	0.41	0.02	17.4	0.82	0.38	0.002
441 base metal	4199474	0.01	0.51	0.37	0.01	17.6	0.08	0.41	0.18
T439Ti wire	ED034209	0.02	0.60	0.60	–	17.5	–	0.01	0.40

Table II

Welding parameters

Sample ID	Shielding gas	Welding speed (mm/s)	Average current (A)	Average welding voltage (V)	Heat input (kJ/mm)
GMAW 441 A	98% Ar–O_2	23.3	122	21	0.12
GMAW 441 B	98% Ar–O_2	16.7	93	20	0.13
GMAW 441 C	98% Ar–O_2	16.7	50	17	0.13
GMAW 441 D	98% Ar–O_2	8.3	50	19	0.08
GTAW 441 E	100% Ar	4.8	60	11	0.13
GTAW 441 1_1	100% Ar	4.8	65	10	0.16
GTAW 441 F	100% Ar	4.8	65	10	0.13
GTAW 441 G	100% Ar	4.8	65	9	0.11
GMAW 436 H	98% Ar–O_2	10.0	56	18	0.11
GMAW 436 I	98% Ar–O_2	10.0	57	18	0.12
GMAW 436 J	98% Ar–O_2	8.3	60	18	0.17
GMAW 436 K	98% Ar–O_2	16.7	117	20	0.16
GTAW 436 L	100% Ar	5.3	75	10	0.19
GTAW 436 M	100% Ar	4.8	75	10	0.14
GTAW 436 N	100% Ar	5.0	75	10	0.15

Table III

Comparison of Ti content, as determined using SEM–EDS and ICP–OES. The carbon and nitrogen contents are also shown

Sample	Ti (%) (SEM)	Ti (%) (ICP)	C (%)(ICP)	N (%) (ICP)
GMAW 441 A [1]	0.51	0.047	0.010	0.0166
GTAW 441 1_1[2]	0.27	0.260	0.015	0.0163
GMAW 436 H[3]	0.52	0.113	0.110	0.0156
GTAW 436 N	0.18	0.069	0.010	0.0160
441 base metal	0.20	0.161	0.024	0.0143
436 base metal	0.00	0.000	0.110	0.0143
T439Ti welding consumable	0.52	0.570	0.027	0.0145

Notes:

[1]CP analysis disregarded – see Figure 2.

[2]Duplicate weld, generated for ICP analysis.

[3]Disregarded – incomplete weld penetration meant that specimen contained base metal and weld metal.

welded joint was generated for image analysis. The maximum dimension of each grain (D_{max}) was determined manually. The maximum dimension perpendicular to D_{max} (D_{min}) and cross-sectional area were then calculated by automated image processing (using ImageJ open-source software). Depending on the fraction of equiaxed grains and grain size on a specific cross-section, between about 130 and 380 grains were measured to fully characterize the cross-section of each welded joint. The results were processed as follows.

- The grain dimension (average of D_{max} and D_{min}) was calculated for each grain and the average dimension for all grains on a cross-section (weighted by the area of each grain on the polished surface) was calculated.
- The distribution of the ratio D_{max}/D_{min}, expressed in terms of the number of grains falling within a specific range of D_{max}/D_{min}, was determined.
- The cumulative area fraction of grains with a D_{max}/D_{min} below a specific value was determined.

Results and discussion

SEM-EDS analysis is considered a semi-quantitative technique, so selected samples covering a range of Ti contents were submitted for ICP–OES analysis. The results are presented in Table III and Figure 2. Two analyses were obviously incorrect and were discarded. From the remaining five analyses, a correction to the

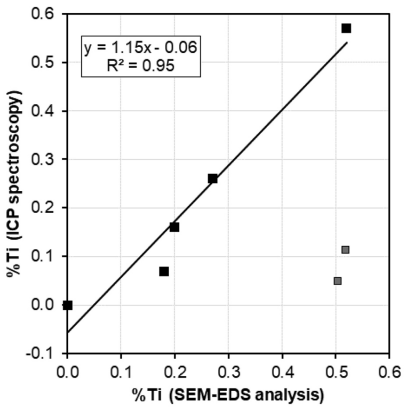

Figure 2—Comparison of Ti content, as determined by SEM–EDS and ICP–OES

SEM–EDS analysis could be defined (as shown in Figure 2). The average of the absolute value of the correction was 0.02% Ti, with a maximum of 0.05% Ti. The corrected values for the Ti content are reported in this document. The C content varied significantly, from about 0.01% to 0.1%; the N content was more stable, with an average of about 150 ppm.

A typical cross-section of a welded joint is shown in Figure 3, with a mixture of long columnar grains and, towards the centre of the weld bead, smaller, more equiaxed grains. The fraction of

Figure 3—Typical cross-section of ferritic stainless steel weld deposited using GMAW (weld GMAW 441 A). The fraction of equiaxed grains is estimated at 0.83 ± 0.10

equiaxed grains was determined using manual point counting: a grid of points was superimposed on an image of the specific weld bead and the number of points falling on equiaxed grains and total number of grains in the weld metal were counted. The fraction of equiaxed grains was estimated from the ratio of the number of points falling on equiaxed grains divided by the total number of points in the weld metal area. The confidence interval was estimated using the equation proposed by Underwood (1970):

$$95\%\ confidence\ interval = \frac{1.96P_p}{\sqrt{P_{EA}}} \quad [1]$$

where P_p and P_{EA} are the fraction and number of points on equiaxed grains, respectively.

Figures 4 to 6 show typical monotone images. Figure 7 shows an example of the results of image processing for the welded joint represented by Figures 3 and 4. The distribution of D_{max}/D_{min}, while relatively easy to interpret, could be skewed by the presence of a small number of very large grains that were sometimes observed in weld metal with low Ti content (see, for example, Figure 5). Calculation of the cumulative area fraction of the welded joint with an increase in D_{max}/D_{min} ratio eliminated this problem; however, quantifying the weld metal microstructure in terms of the D_{max}/D_{min} ratio for each grain did not distinguish between large grains and small grains. Furthermore, using a parameter based on D_{max}/D_{min} did not permit comparison of the results of this study with previous work. The fraction of equiaxed grains therefore proved to be the most suitable parameter to describe the weld metal microstructure.

Results for the fraction of equiaxed grains (as determined using point counting) and Ti content (measured using SEM-EDS and corrected according to the ICP analyses) are presented in Table IV and Figure 8. Published data (Figure 1) is included in Figure 8 for ease of comparison. A wide range of weld metal Ti contents was achieved. There was no apparent difference in the fraction of equiaxed grains in the weld metal for GTAW and GMAW beads for similar Ti contents. The fraction of equiaxed grains gradually increased with a higher Ti content, up to approximately 0.4% Ti; above this value, the fraction of equiaxed grains in the weld metal increased rapidly and non-linearly, reaching a plateau of approximately 0.80. Given the wide range of welding speeds used, the consistency of the fraction of equiaxed grains in the weld metal was unexpected: the Ti content apparently dominated the CET in these steels. Villaret

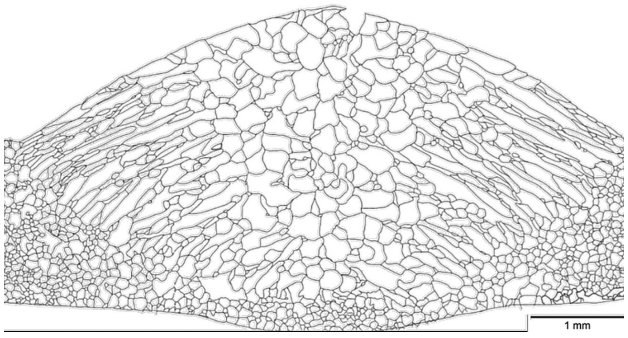

Figure 4—Grain boundaries of ferritic stainless steel weld shown in Figure 3 (weld GMAW 441 A)

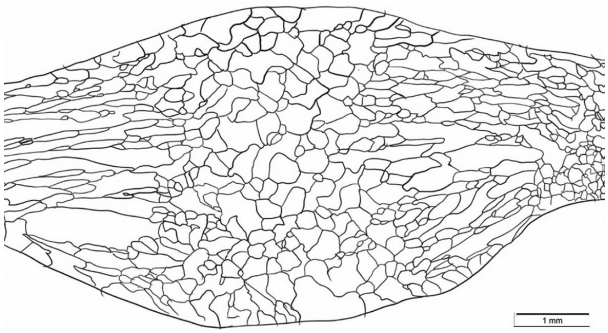

Figure 6—Grain boundaries of a GTAW bead in Type 441 ferritic stainless steel, containing about 0.5% Ti (weld GTAW 441 D). The fraction of equiaxed grains is estimated at 0.47 ± 0.06

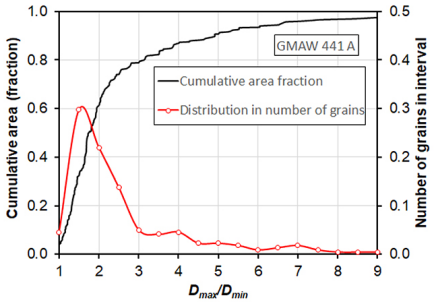

Figure 7—Distribution in ratio of major to minor grain dimensions (D_{max}/D_{min}) and cumulative distribution (expressed in terms of surface area) in ratio (D_{max}/D_{min}) for the weld shown in Figure 3 and 4 (Weld 441 A)

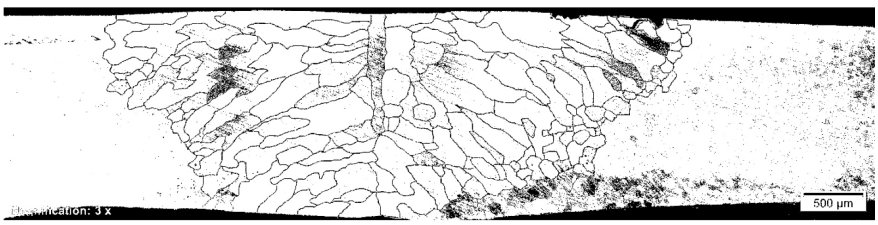

Figure 5—Grain boundaries of an autogenous weld in Type 436 ferritic stainless steel, containing very little Ti and a low fraction of equiaxed grains (GTAW 436 L)

Table IV

Fraction of equiaxed grains (determined using manual point counting) and Ti content of weld metal. SEM–EDS analysis of Ti content was corrected by reference to ICP data

Sample ID	Number of points in equiaxed grains	Total number of points	Estimated fraction equiaxed grains	Measured Ti (%) (SEM–EDS)	Corrected Ti content (%)
GMAW 441 A	288	346	0.83 ± 0.10	0.51	0.52
GMAW 441 B	332	480	0.69 ± 0.07	0.45	0.46
GMAW 441 C	259	472	0.55 ± 0.07	0.44	0.45
GMAW 441 D	247	528	0.47 ± 0.06	0.41	0.41
GTAW 441 E	60	459	0.13 ± 0.03	0.21	0.18
GTAW 441 1_1	67	412	0.16 ± 0.04	0.27	0.25
GTAW 441 F	102	450	0.23 ± 0.04	0.38	0.38
GTAW 441 G	62	320	0.19 ± 0.05	0.22	0.20
GMAW 436 H	473	570	0.83 ± 0.07	0.52	0.54
GMAW 436 I	129	477	0.27 ± 0.05	0.37	0.37
GMAW 436 J	83	434	0.19 ± 0.04	0.30	0.29
GMAW 436 K	141	636	0.22 ± 0.04	0.33	0.33
GTAW 436 L	0	495	0	0.00	0.00
GTAW 436 M	31	480	0.06 ± 0.02	0.07	0.02
GTAW 436 N	45	220	0.20 ± 0.06	0.18	0.15

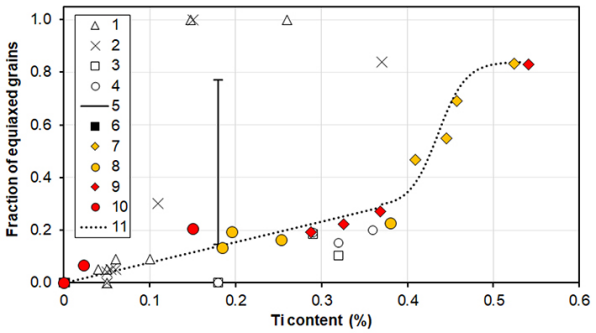

Figure 8—Change in fraction of equiaxed grains as a function of Ti content (key to data: 1: pulsed GMAW, Villaret, *et al.*, 2013a; 2: short circuit GMAW, Villaret *et al.*, 2013a; 3: GTAW 3 mm/s Villafuerte, Pardo, and Kerr, 1990; 4: GTAW 14 mm/s Villafuerte *et al.*, 1990; 5: Grade 441 Prins, 2020, 6: Grade 436: Prins, 2020; 7: current study GMAW 441; 8: current study GTAW 441; 9: current study GMAW 436; 10: GTAW 436; 11: interpolation of current results)

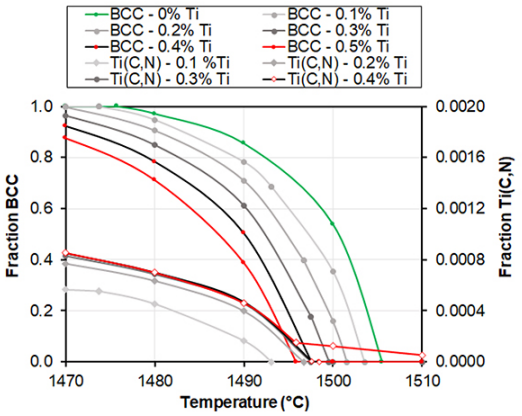

Figure 9—Changes in ferrite (body-centred cubic, BCC) and Ti(C,N) phases as a function of temperature under equilibrium conditions, estimated using Thermo-Calc, for hypothetical chemical compositions based on Type 441 stainless steel with 0%, 0.3%, 0.4%, and 0.5% Ti

et al. (2013a) reported a high fraction of equiaxed grains in Type 444 weld metal with more that 0.15% Ti, well below the 0.4% Ti observed during the current study. The Type 444 weld metal also contained 19% Cr, 2% Mo, and between 0.21 and 0.71% Nb. The low Ti content that is necessary to achieve a high fraction of equiaxed grains in 444 weld metal may be related to the high Nb content and the associated wider solifidifcation range (Konadu and Pistorius, 2021); this argument is explored in more detail below.

Possible reasons for the effect of Ti on the solidification structure were explored using Thermo-Calc software to estimate the amounts of specific phases present at a given temperature under equilibrium conditions. A weld pool, especially the very small weld pools encountered in the current study, cools down very rapidly, so solidification and solid-state phase transformations occur under conditions far from equilibrium. However, the equilibrium conditions represent a first-order approximation of the likely sequence of phase transformations. The chemical composition of Type 441 ferritic stainless steel (Table I) was used for the Thermo-Calc estimates. The Ti content was varied from zero to 0.5% Ti, which covered the full range of Ti contents encountered in this study. The results, summarized in Figure 9, show the ferrite and Ti(C,N) contents as a function of temperature from 0% to 0.5% Ti. Higher Ti content resulted in a gradual decrease in the liquidus temperature (the temperature at which the first ferrite forms during solidification) and solidus temperature (the temperature at which the last liquid disappears on cooling, not shown). As the Ti content increased, the Ti(C,N) content at a specific temperature did not increase significantly until approximately 0.5% Ti. At approximately 0.4% Ti, the liquidus temperature (the temperature at which the formation of ferrite from the liquid metal becomes thermodynamically possible) is similar to the temperature at which the first Ti(C,N) becomes thermodynamically stable on cooling. If Ti-rich precipitates were present at or above the liquidus temperature, heterogenous nucleation of ferrite on Ti(C,N) precipitates and the associated formation of equiaxed grains would be thermodynamically possible. The Thermo-Calc estimates for the changes in fractions of ferrite and Ti(C,N) with temperature were therefore consistent with the abrupt change in the fraction of equiaxed grains as the Ti content of the weld metal increased.

The validity of using equilibrium data to estimate the minimum Ti content in a weld metal required to achieve equiaxed

grains was verified by reviewing the data for the five Type 409 steels reported by Villafuerte, Pardo, and Kerr (1990), shown in Figure 10. With one exception (a welding speed of 14 mm/s), equiaxed grains were only present if the weld metal contained more than 0.2% Ti, and usually more than 0.28% Ti. The average chemical composition of these steels was calculated as (%) 11.2 Cr, 0.24 Ni, 0.009 C, 0.03 Al, 0.40 Mn, 0.45 Si. A Thermo-Calc estimate of the fractions of ferrite and Ti(C,N) as a function of temperature for this steel was calculated for variation in Ti content from 0.1% to 0.4% in 0.1% Ti increments. The results of these calculations are shown in Figure 11. Similar to the behaviour of Type 441 weld metal, the fraction of equiaxed grains started to increase only once the Ti content was high enough that, under equilibrium conditions, Ti(C,N) precipitates were present at the liquidus temperature. The difference in the minimum amount of Ti necessary for the formation of a significant fraction of equiaxed grains in the weld metal between Type 441 (approximately 0.4% Ti) and Type 409 (0.2%–0.3% Ti) is therefore related to the liquidus temperature and stability of the Ti(C,N) precipitate.

The implication of the results of the current study is that a minimum Ti content is necessary for a ferritic stainless steel weld to contain a substantial proportion of equiaxed grains. The minimum amount of Ti necessary to achieve a substantially equiaxed structure is sensitive to the chemical composition of the specific grade of stainless steel: for Types 436 and 441, at least 0.4% Ti must be present in the weld metal to achieve a substantially equiaxed structure. The weld metal Ti content can be present in the base metal and an autogenous weld may be used. If a Ti-containing welding consumable is used, the Ti content of the weld metal can be considerably higher than that of the base metal. The high dilution (fraction of weld metal contributed by melting of the base metal) inherent in GTAW limits the maximum Ti content and therefore the fraction of equiaxed grains; if GMAW is used, weld metal with a high Ti content and a high fraction of equiaxed grains can be achieved.

Conclusions

- For the weld metal characterized in this study, the fraction of equiaxed grains in a ferritic stainless weld is dependent on the Ti content, but is not sensitive to the welding process.
- The use of SEM-EDS resulted in a reasonably accurate determination of the Ti content of the weld metal, with a correction (based on ICP-OES analyses) that did not exceed 0.05% Ti.
- The Ti content of the weld metal was determined by the Ti content of the base metal, the degree of dilution (dependent on the welding process used), and whether a Ti-containing welding consumable was used.
- The response of the fraction of equiaxed grains to an increase in the Ti content of the weld metal was characterized by a gradual increase in the fraction of equiaxed grains up to a specific Ti content; above that value, the fraction of equiaxed grains increased rapidly with increasing Ti content. Thermodynamic modelling indicated that the transition in behaviour correlated with a Ti content at which some Ti(C,N) was stable at the predicted liquidus of the weld metal.

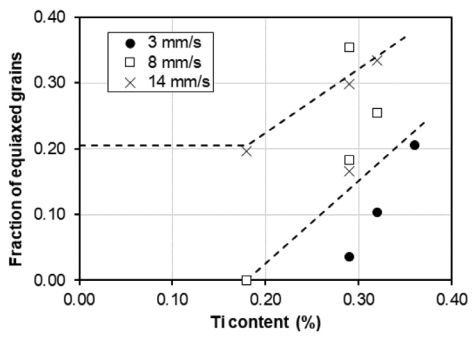

Figure 10—Data reported by Villafuerte, Pardo, and Kerr (1990) for the fraction of equiaxed grains observed on the surface of Type 409 stainless steel welds as a function of Ti content. The dotted lines are as proposed by Villafuerte, Pardo, and Kerr (1990)

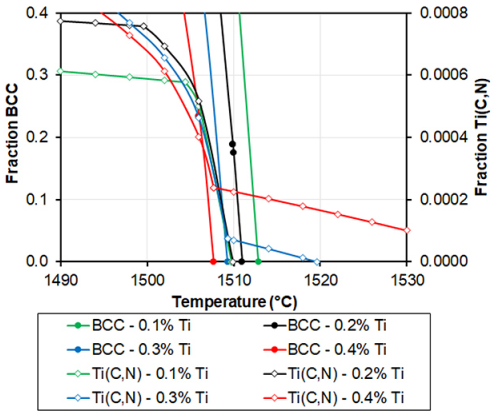

Figure 11—Changes in ferrite (body-centred cubic, BCC) and Ti(C,N) phases as a function of temperature under equilibrium conditions, estimated using Thermo-Calc, for hypothetical chemical compositions based on the average composition of Type 409 steels reported by Villafuerte Pardo, and Kerr (1990), with the Ti content as indicated

Acknowledgements

The Southern African Institute of Welding and Columbus Stainless provided financial support. Studies by several undergraduate students on the welding of ferritic stainless steels in recent years are recognized. S.S. Mahlalela contributed the Thermo-Calc data.

References

Konadu, D.S. and Pistorius, P.G.H. 2021. Investigation of formation of precipitates and solidification temperatures of ferritic stainless steels using differential scanning calorimetry and Thermo-Calc simulation. *Sādhanā*, vol. 46, no. 3. pp. 1–8.

Lippold, J.C. 2014. Welding Metallurgy and Weldability. Wiley.

Prins, H.J. 2020. The effects of autogenous gas tungsten arc welding parameters on the solidification structure of two ferritic stainless steels. MEng thesis, University of Pretoria, South Africa.

Underwood, E.E. 1970. Quantitative Stereology. Addison Wesley, Reading. p. 23.

Villafuerte, J.C., Pardo, E., and Kerr, H.W. 1990. The effect of alloy composition and welding conditions on columnar-equiaxed transitions in ferritic stainless steel gas-tungsten arc welds. Metallurgical Transactions A, vol. 21, no. 7. pp. 2009–2019.

Villafuerte, J.C., Kerr, H.W., and David, S.A. 1995. Mechanisms of equiaxed grain formation in ferritic stainless steel gas tungsten arc welds. *Materials Science and Engineering A*, vol. 194, no. 2. pp. 187–191.

Villaret, V., Deschaux-Beaume, F., Bordreuil, C., Rouquette, S., and Chovet, C. 2013a. Influence of filler wire composition on weld microstructures of a 444 ferritic stainless steel grade. *Journal of Materials Processing Technology*, vol. 213, no. 9. pp. 1538–1547. https://doi.org/10.1016/j.jmatprotec.2013.03.026

Villaret, V., Deschaux-Beaume, F., Bordreuil, C., Fras, G., Chovet, C., Petit, B., and Faivre, L. 2013b. Characterization of gas metal arc welding welds obtained with new high Cr–Mo ferritic stainless steel filler wires. *Materials & Design*, vol. 51. pp. 474–483. https://doi.org/10.1016/j.matdes.2013.04.054

Villaret, V., Deschaux-Beaume, F., and Bordreuil, C. 2016. A solidification model for the columnar to equiaxed transition in welding of a Cr-Mo ferritic stainless steel with Ti as inoculant. *Journal of Materials Processing Technology*, vol. 233. pp. 115–124. https://doi.org/10.1016/j.jmatprotec.2016.02.017 ◆